

# Complexation of Phenols and Thiophenol by Phosphine Oxides and Phosphates. Extraction, Isothermal Titration Calorimetry, and *ab Initio* Calculations

Ruud Cuypers,<sup>†</sup> Bernhard Burghoff,<sup>‡</sup> Antonius T. M. Marcelis,<sup>†</sup> Ernst J. R. Sudhölter,<sup>†,§</sup> André B. de Haan,<sup>\*,‡</sup> and Han Zuilhof<sup>\*,†</sup>

Laboratory of Organic Chemistry, Wageningen University, Dreijenplein 8, 6703 HB Wageningen, The Netherlands, Department of DelftChemTech, Delft University of Technology, Julianalaan 136, 2628 BL Delft, The Netherlands, and Chemical Engineering and Chemistry Process Systems Engineering, Eindhoven University of Technology, P.O. Box 513, 5600 MB Eindhoven, The Netherlands

Received: February 23, 2008; Revised Manuscript Received: September 20, 2008

To develop a new solvent-impregnated resin system for the removal of phenols from water the complex formation of triisobutylphosphine sulfide (TIBPS), tributylphosphate (TBP), and tri-*n*-octylphosphine oxide (TOPO) with a series of phenols (phenol, thiophenol, 3-chlorophenol, 3,5-dichlorophenol, 4-cyanophenol, and pentachlorophenol) was studied. The investigation of complex formation between the extractants and the phenols in the solvent toluene was carried out using liquid–liquid extraction, isothermal titration calorimetry (ITC), and quantum chemical modeling (B3LYP/6-311+G(d,p)//B3LYP/6-311G(d,p) and MP2/6-311++G(2d,2p)//B3LYP/6-311G(d,p)). The equilibrium constant (binding affinity,  $K_{\text{chem}}$ ), enthalpy of complex formation ( $\Delta H$ ), and stoichiometry ( $N$ ) were directly measured with ITC, and the entropy of complexation ( $\Delta S$ ) was derived from these results. A first screening of  $K_{\text{chem}}$  toward phenol revealed a very high binding affinity for TOPO, and very low binding affinities for the other extractants. Modeling results showed that although 1:1 complexes were formed, the TIBPS and TBP do not form strong hydrogen bonds. Therefore, in the remainder of the research only TOPO was considered.  $K_{\text{chem}}$  of TOPO for the phenols in toluene increased from 1 000 to 10 000  $\text{M}^{-1}$  in the order phenol < pentachlorophenol < 3-chlorophenol < 4-cyanophenol  $\approx$  3,5-dichlorophenol (in line with their  $\text{p}K_{\text{a}}$  values, except for pentachlorophenol) in the absence of water, while the stoichiometric ratio remained 1:1. In water-saturated toluene, the binding affinities are lower due to co-complexation of water with the active site of the extractant. The increase in binding affinity for TOPO in the phenol series was confirmed by a detailed *ab initio* study, in which  $\Delta H$  was calculated to range from  $-10.7$  kcal/mol for phenol to  $-13.4$  kcal/mol for 4-cyanophenol. Pentachlorophenol was found to behave quite differently, showing a  $\Delta H$  value of  $-10.5$  kcal/mol. In addition, these calculations confirm the formation of 1:1 H-bonded complexes.

## Introduction

Solvent-impregnated resins<sup>1</sup> (SIRs, Figure 1) are used as three-phase separation systems. A solute is present in an aqueous phase; the SIR contains the stationary, diluent phase, an organic liquid impregnated in the pores of the inert resin particle. When brought in contact with a SIR, the solute will diffuse from the aqueous phase into the diluent phase, with equilibrium constant  $K_{\text{phys}}$ . Ion-exchange SIRs are already widely used to separate heavy metal ions<sup>2–11</sup> from aqueous phases in a fast and simple way, making use of the solubility of the solute in the liquid organic phase, in exchange for protons. Only recently have other applications been investigated, e.g., the large-scale recovery of apolar organics<sup>12</sup> and bench-scale or pilot-scale recovery of polar organics like organic acids,<sup>13,14</sup> amino acids,<sup>15</sup> and flavonoids.<sup>16</sup> However, large-scale applications for the separation of polar solutes, like ethers and phenols, do not yet exist.

SIRs display general advantages when compared to other separation techniques. While during conventional extraction

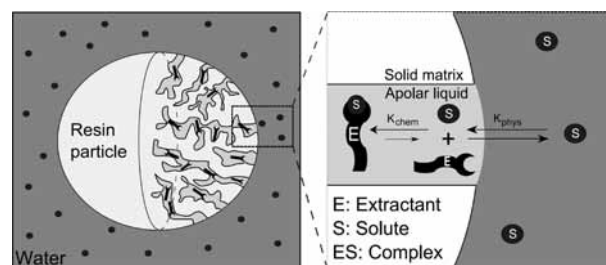


**Figure 1.** Operational principle of solvent-impregnated resins with an active extracting agent in the pores.

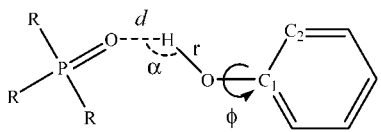
(liquid–liquid extraction) the solvent and the extractant have to be dispersed, in a SIR setup the dispersion is already achieved by the impregnated particles. This also removes the requirement of an additional phase-separation step. In addition, the impregnation step decreases solvent loss.<sup>17</sup> Furthermore, SIRs have a crucial advantage over, e.g., ion-exchange resins with chemically bound extractants, as they can be reused for different separation tasks by simply rinsing one extractant out and reimpregnating them with another one, thereby saving expensive resin design and production. A SIR system works well for highly apolar solutes,<sup>1</sup> but to adequately separate more polar organic compounds from aqueous streams, improved extraction is required. To enhance extraction, complex-forming extractants can be

\* Corresponding authors. A.B.deH.: Eindhoven University of Technology, phone +31-40-2475259, fax +31-40-2463966, e-mail a.b.dehaan@tue.nl. H.Z.: Wageningen University, phone +31-317-482367, fax +31-317-484914, e-mail han.zuilhof@wur.nl.

<sup>†</sup> Wageningen University.

<sup>‡</sup> Delft University of Technology.

<sup>§</sup> Eindhoven University of Technology.

**TABLE 1: Compounds under Investigation in the Calculations, and Angular and Radial Parameters Describing H-Bond Geometry in Phosphine Oxides and Phosphates<sup>a</sup>**


compd	molecular formula
phenol	C <sub>6</sub> H <sub>5</sub> OH (1)
thiophenol	C <sub>6</sub> H <sub>5</sub> SH (2)
3-chlorophenol	3-Cl-C <sub>6</sub> H <sub>4</sub> OH (3)
3,5-dichlorophenol	3,5-Cl <sub>2</sub> -C <sub>6</sub> H <sub>3</sub> OH (4)
4-cyanophenol	4-CN-C <sub>6</sub> H <sub>4</sub> OH (5)
pentachlorophenol	Cl <sub>5</sub> -PhOH (6)
phosphates	O=PR <sub>3</sub> (R = -O-CH <sub>3</sub> ) (7)
thiophosphates	S=PR <sub>3</sub> (R = -O-CH <sub>3</sub> ) (8)
phosphine oxides	O=PR <sub>3</sub> (R = -CH <sub>2</sub> -CH <sub>3</sub> ) (9)
phosphine sulfides	S=PR <sub>3</sub> (R = -CH <sub>2</sub> -CH <sub>3</sub> ) (10)

<sup>a</sup> H-bond length,  $d$  (Å), H-bond angle,  $\alpha$  (deg), O-H bond length,  $r$  (Å), and dihedral angle between C1 and C2 respectively, and  $r$ ,  $\phi$  (deg).

added to the diluent. By means of complex formation, with equilibrium constant  $K_{\text{chem}}$ , the overall equilibrium concentration of solute in the diluent phase can, in principle, be increased, in which case the overall extraction would be significantly enhanced. An optimization of the complex-forming ability of the extractant (high  $K_{\text{chem}}$ ) can thus improve the SIRs performance.<sup>18</sup>

In principle, molecular recognition and complexation of the solute inside the SIR particles, as indicated in Figure 1, can provide a new and fast way to separate more polar organic solutes from aqueous streams. Ultimately, the extractant itself should possess a low melting point and be a liquid at room temperature, so that a diluent would no longer be necessary. A high boiling point would also be beneficial, because it facilitates regeneration at elevated temperatures. For the effective removal of polar and protic organic solutes like ethers and phenols, as e.g. desired in water-cleaning processes, the additional complexation step of the solute in the diluent phase turns out to be crucial for large-scale application, due to the relatively high solute solubility in water. The current techniques of phenol extraction include common liquid-liquid extraction, membrane-based solvent extraction in coupled ultrafiltration modules,<sup>19</sup> and hollow fiber modules.<sup>20</sup> Also, dual-solvent extraction processes are used to recover organic pollutants from water, but these are very energy-consuming and can lead to contamination of the wastewater with the polar extractant.<sup>21</sup> Therefore, an extractant-impregnated resin approach is currently under development in our laboratories.

The basis for optimizing an extractant via molecular design is a deeper understanding at the molecular level. Molecular modeling can facilitate this understanding by providing useful data about the complexation processes. The results of the modeling experiments can then be compared with experimental data. In this paper we investigate a set of extractants for the extraction of phenol, thiophenol, and substituted phenols from an aqueous environment, to establish the basis for a future industrial design. Strong hydrogen bonds are desired for SIR-based processes, which prompted this study with phosphates and phosphine oxides that can form hydrogen-bonding complexes with phenols<sup>22</sup> (Table 1). Alkylated phosphates and phosphine oxides combine a low solubility in water with a partial

negative charge on the oxygen atom that was expected to be favorable for hydrogen bonding. The most important hydrogen bond characteristics to be explored in this paper are the hydrogen bond strength and the geometry of the resulting complexes. From literature, neutral O-H...O hydrogen bonds are expected to have a strength of ca. 5 kcal/mol<sup>22,23</sup> covering a range of H-bond lengths and O-H...O angles,<sup>24,25</sup> as these parameters depend strongly on the molecular geometry of the system at hand. The interaction between the phenols and the extractants is investigated in detail experimentally with liquid-liquid extraction experiments and isothermal titration calorimetry (ITC). Although a great deal of information about hydrogen bonding of phenols by phosphates and phosphine oxides is already available from the literature,<sup>22,26-33</sup> this information was obtained from measurements in CCl<sub>4</sub>. Most of the results obtained in these literature reports are based on IR measurements and subsequent derivation of the thermodynamic parameters. Due to the experimental complexity and the assumptions that have to be made, no consistency in the results exists in the literature, as has also been pointed out elegantly by Jeffrey.<sup>22</sup> In addition, we report for the first time complexation constants obtained in water-saturated toluene to quantify the effect of water on complexation constants when measured in an environment that contains water. These literature reports are therefore different and unsuitable for our purposes, i.e., for understanding the factors essential to the development of a solvent-impregnated resin extraction system for removal of phenols from an aqueous system. Results obtained on different systems cannot be compared directly, as is clear from our results for pentachlorophenol complexation by phosphine oxide (vide infra). Where some investigators<sup>26,32</sup> find lower complexation constants for pentachlorophenol compared to phenol, we now report higher complexation constants for the former, based on both ITC measurements and molecular modeling in vacuo.

Liquid-liquid extraction experiments are used to test phosphate, phosphine sulfide, and phosphine oxide extractants in two-phase systems for their potential in phenol extraction. With these experiments, the overall distribution coefficients  $K_D$  are obtained. In addition, ITC measurements were performed to get insight into the binding affinity  $K_{\text{chem}}$ , and to obtain the thermodynamic data involved in complex formation. ITC<sup>34-38</sup> can be used to directly measure the binding affinity (equilibrium constant,  $K_{\text{chem}}$ ) and thermodynamic parameters (enthalpy of complex formation,  $\Delta H$ , and stoichiometry,  $N$ ) in complexation reactions, and the values of change in entropy,  $\Delta S$ , and free energy,  $\Delta G$ , can be derived from this. Although by far most of the ITC measurements reported in literature are carried out in aqueous solutions, its use is also unproblematic with cosolvents such as methanol or DMSO,<sup>39</sup> or with organic solvents such as chloroform,<sup>40,41</sup> toluene,<sup>41-43</sup> or others.<sup>44</sup> The reasons to use toluene in our experiments include first of all its utility as a model system for the industrial application of SIRs that we are aiming for (in contrast to CCl<sub>4</sub>, which is a probable carcinogen). In addition, toluene presents only a minor influence on hydrogen bonding interactions, and it is a good solvent for the compounds that are under investigation. Many investigations on hydrogen bonding describe experimental work that is carried out in toluene, and clearly indicate that this solvent does not affect hydrogen bond formation much.<sup>45-47</sup> Hydrogen bonds in all kinds of systems have been extensively studied by density functional theory.<sup>23,24,48-53</sup> In this work, molecular modeling experiments have been applied to investigate the complex formation. The geometries of the monomers and complexes have all been optimized at the B3LYP/6-311G(d,p) level of theory,

which generally describes the geometries of these systems well. Two different high-level methods (B3LYP/6-311+G(d,p)//B3LYP/6-311G(d,p) and MP2/6-311++G(2d,2p)//B3LYP/6-311G(d,p), including counterpoise correction for MP2) in combination with an SCRF approach to mimic the solvent effects of toluene were used to obtain energy data and other properties that are not too dependent on the method used. Although analysis of a small data set of hydrogen-bonded complexes suggests that other density functionals might perform somewhat better in describing hydrogen-bonding interactions,<sup>54</sup> no analysis has been presented in the literature that includes a series of compounds with sulfur or phosphor atoms, and therefore the widely used B3LYP functional was used here. In the resulting analysis the theoretical predictions and the experimentally obtained results have been combined to provide a detailed picture and insight into the complexing behavior of phenols toward several phosphates and phosphine oxides.

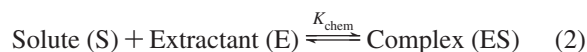
## Experimental Section

**General.** The following materials were used as received without further purification: tri-*n*-octylphosphine oxide (TOPO) ( $\geq 99\%$ , Sigma Aldrich), Cyanex 923 (a mixture of four trialkylphosphine oxides  $R_3PO$ ,  $R_2R'PO$ ,  $RR'_2PO$ , and  $R'_3PO$ , where  $R = n-C_6H_{13}$  and  $R' = n-C_8H_{17}$ ; 93%, Cytec Industries), tri-*n*-butylphosphate (TBP) ( $>99\%$ , Merck), triisobutylphosphine sulfide (TIBPS) (98%, Cytec Industries), phenol ( $>99\%$ , Merck), 3-chlorophenol (99%, Janssen Chimica), 3,5-dichlorophenol (99%, Sigma Aldrich), 4-cyanophenol (95%, Sigma Aldrich), pentachlorophenol (99%, Sigma Aldrich), and thiophenol (97%, Janssen Chimica). All ITC measurements were performed with p.a.-quality toluene dried on molecular sieves (3 Å).

**Liquid–Liquid Extraction.** In a SIR system, in equilibrium the overall distribution coefficient  $K_D$  is defined as described in eq 1. The concentration of solute in the organic phase (extractant and diluent) based on partitioning is  $c_S^{org}$ , the concentration of the complex in the organic phase is  $c_{ES}^{org}$ , and the concentration of the solute in the aqueous phase is  $c_S^{aq}$ .

$$K_D = \frac{c_S^{org} + c_{ES}^{org}}{c_S^{aq}} \quad (1)$$

The amount of solute in the pores of the SIR particle consists of dissolved solute and complexed solute. The extraction is mainly based on the binding affinity  $K_{chem}$  (vide infra), in this case resulting from the hydrogen bond formation between the extractant and the solute. This chemical equilibrium inside the pores of the SIR particle can be described via



Thus,  $K_{chem}$  is derived as in eq 3. The equilibrium concentration of the extractant in the organic phase is represented by  $c_E^{org}$ .

$$K_{chem} = \frac{c_{ES}^{org}}{c_S^{org} \cdot c_E^{org}} \quad (3)$$

The partitioning of phenol between the aqueous phase and the organic phase inside the resin particle is given in eq 4.

$$K_{phys} = \frac{c_S^{org}}{c_S^{aq}} \quad (4)$$

Inserting eqs 3 and 4 into eq 1 gives eq 5, an expression of the overall distribution coefficient  $K_D$ , depending on the physical and chemical equilibrium constants.

$$K_D = K_{phys} + K_{phys} \cdot K_{chem} \cdot c_E^{org} \quad (5)$$

This correlation can also be represented in a graph (Figure 2), which can be used to determine conveniently the influence of both physical and chemical extraction.

In the extraction experiments aqueous solutions (presaturated with toluene) of 40 g of demineralized water containing 1000 ppm w/w phenol (a typical concentration in large-scale extractions) were mixed with 4 g of extractant solution. The extractant solutions (0.1, 0.5, 1.0, and 1.5 M) were prepared by dissolving either TOPO, Cyanex 923, TBP, or TIBPS in toluene (presaturated with water; the mole fraction solubility of water in toluene at 30 °C is around 0.003,<sup>55–57</sup> i.e.  $[H_2O] \approx 28$  mM). Toluene itself has only a very low capacity for phenol (vide infra), which is the reason why it was chosen as a diluent. Toluene, with no extractant dissolved, was also used to extract phenol, in order to determine the physical partitioning of phenol in the extractant solution ( $K_{phys}$ ). The extraction vessels were stirred at 500 rpm for  $\geq 16$  h at a constant ambient temperature of 30 °C. Afterward, the two phases were separated. Samples of the aqueous phase were filtered with two 0.2  $\mu\text{m}$  filter units (Whatman Spartan 30/0.2 RC). Samples of 1–10 mL of the aqueous phase were diluted with demineralized water to give a volume of 100 mL. After this, successively 5 mL of buffer solution pH 10 (ammonia 25%, ammonium chloride, potassium sodium tartrate–tetrahydrate, water), 3 mL of potassium hexacyanoferrate solution, and 3 mL of 4-aminoantipyrine solution (4-amino-2,3-dimethyl-1-phenyl-3-pyrazolin-5-one, water) (all according to DEV H 16) were added. According to the Emerson reaction<sup>58,59</sup> the phenol was complexed by 4-aminoantipyrine and this complex was detected with a Varian Cary 300 UV/vis spectrophotometer at 510 nm. The equilibrium concentration of phenol in the aqueous phase was calculated by using a calibration line; the equilibrium concentration of phenol in the organic phase was calculated from the mass balance. From these concentrations the overall distribution coefficient ( $K_D$ ) was calculated.

**Isothermal Titration Calorimetry (ITC).** ITC was performed on a MicroCal VP-ITC microcalorimeter; the setup is described elsewhere.<sup>60</sup> Results were processed using Origin 7SR2 V7.0383 (B383) by Origin Laboratory Corporation. The measuring cell (1.46 mL) was flushed and filled with a freshly prepared and degassed solution of the phenolic compound in either carefully dried toluene (usually concentrations between 1 and 10 mM were used) or toluene that was saturated with water. The 280  $\mu\text{L}$  automatic syringe was flushed and filled with a freshly prepared and degassed solution of the complexing agent in dry toluene at a concentration of roughly 10 times the molarity of the cell solution. Depending on the concentration of the compounds in solution and the magnitude of the heat effect per second, the number of injections and the injected volume per injection were chosen. Between subsequent injections a sufficient amount of time was chosen to allow for the cell feedback to return to the baseline, usually 180 to 300 s. Stirring speed for all ITC measurements was 502 rpm (default value). A reference measurement was performed using the same procedure, only having the solvent, not the solute, in the measuring cell. By subtracting the reference measurement from the actual measurement the net results were obtained and they were fitted using the one-set-of-sites model present in the Origin software.

**Modeling.** Computational data were all obtained using the Gaussian03 suite of programs.<sup>61</sup> All B3LYP/6-311G(d,p)-optimized stationary points were confirmed as true minima via vibrational frequency calculations. This was followed by single-



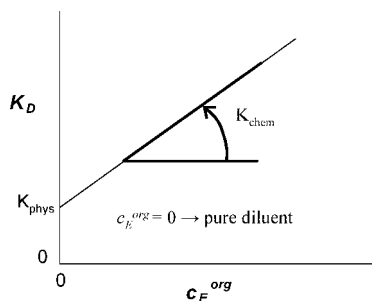


**Figure 2.** Graphical representation of the overall distribution coefficient with the physical and chemical equilibrium constants,  $K_{\text{phys}}$  and  $K_{\text{chem}}$ , respectively.

point calculations of the optimized geometries at the B3LYP/6-311+G(d,p) and MP2/6-311++G(2d,2p) levels of theory. These two methods were chosen to ensure that results are not influenced by method-dependent phenomena, and basis sets were chosen big enough to ensure sufficient accuracy.<sup>53,62</sup> It is known that at this level B3LYP yields accurate energy data in many cases, specifically for minimum energy structures, although hydrogen bond lengths are generally a little underestimated.<sup>63</sup> MP2 performs at this level typically well both in geometry optimization as well as in estimation of interaction energies for hydrogen bonding.<sup>49,52,63</sup>

In an effort to reproduce the experimental results as accurately as possible, the effect of the medium (toluene) was also simulated, using the self-consistent reaction field (SCRf) method in the polarizable continuum model (PCM) at the B3LYP/6-311+G(d,p) level.<sup>64</sup> For these calculations the solvent “toluene” was specified in the input section. Finally, since electrostatic interactions are crucial for the strength of hydrogen bonds,<sup>65–69</sup> natural population analysis (NPA)<sup>70,71</sup> charges were obtained, as these display a relatively small method and basis set dependence and have proven to be reliable charge indicators for related theoretical studies of hydrogen bonds. In addition, atom–atom overlap-weighted natural atomic orbital (NAO) bond orders were obtained.

Specifically MP2 calculations of hydrogen bonding interactions are subject to a basis set superposition error (BSSE) because of over-stabilization due to the supermolecular approach.<sup>72</sup> An a posteriori counterpoise (CP)<sup>73,74</sup> BSSE correction has therefore been used (MP2 only), and a zero-point correction to the energy was applied.

Complexes that were investigated in this way each consisted of a phenol or thiophenol, and one of the phosphates/phosphine oxides (Table 1). The model compounds resemble the compounds used in liquid–liquid extraction experiments and ITC, but for computational speed the long alkyl tails were replaced by methyl or ethyl groups. In Table 1 the different relevant geometrical parameters are defined for hydrogen bonds in the investigated complexes.

## Results and Discussion

**Liquid–Liquid Extraction.** The physical equilibrium constant ( $K_{\text{phys}}$ ) is determined by the partitioning of phenol in the inert diluent toluene, and amounts to 1.5 at 30 °C. The chemical equilibrium constant ( $K_{\text{chem}}$ ) is dependent on the extractant dissolved in the toluene. As can be seen in Table 2,  $K_{\text{phys}}$  is very low compared to  $K_{\text{chem}} \times c_E$ . Therefore, the extraction is dominated by the chemical interaction of phenol with the respective extractant dissolved in the toluene phase. Table 2 also shows that the trialkylphosphine oxides TOPO and Cyanex 923 have the highest overall distribution coefficients  $K_D$  in the

**TABLE 2: Chemical Equilibrium Constants,  $K_{\text{chem}}$  ( $\text{M}^{-1}$ ), Calculated from Overall Distribution Coefficients,  $K_D$ , Determined by Liquid–Liquid Extraction of Phenol**

extractant	$c_E^{\text{org}}$ [M]	$K_D$	$K_{\text{chem}}$ [ $\text{M}^{-1}$ ]
toluene	0.00	1.5 <sup>a</sup>	0
Cyanex 923	0.10	25	551
	0.51	397	
	1.00	677	
	1.56	883	
TOPO	0.10	29	579
	0.50	374	
	1.00	689	
	1.50	791	
TBP	0.10	11	77
	0.47	56	
	0.94	101	
	1.44	148	
TIBPS	0.51	6	5
	1.01	7	
	1.50	11	

<sup>a</sup> Equals  $K_{\text{phys}}$ .

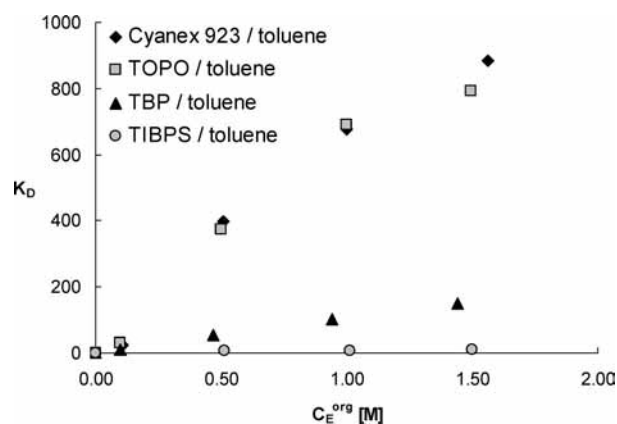


**Figure 3.** Overall distribution coefficients,  $K_D$ , determined by liquid–liquid extraction of phenol.

liquid–liquid extraction experiments, compared to the other substances, which is also graphically shown in Figure 3.

On the basis of the higher polarity of the phosphate group as compared to the phosphine oxide group, one might have expected a higher phenol distribution coefficient  $K_D$  for tributylphosphate (TBP) than for Cyanex 923 or TOPO. However, the  $K_D$  of TBP is found to be significantly lower. A likely reason for this is the coextraction of water by TBP from the aqueous phase. This plays a bigger role for TBP than for, e.g., TOPO, due to the significantly longer alkyl chains of TOPO, which makes the overall local medium for the complexed water much less polar. It is also seen that the tested triisobutylphosphine sulfide (TIBPS) is a less effective phenol extractant than the trialkylphosphine oxides and the trialkylphosphate. The lower electron density at the sulfur in the phosphine sulfide group (see Natural Population Analysis data, vide infra) makes it a weaker hydrogen bond acceptor, and therefore a weaker extractant.

For the application in SIRs it would be desirable to work without diluents like toluene to avoid a contamination of the aqueous phase with the diluent, and to achieve a higher concentration of extractant inside the SIR. Cyanex 923 would therefore be the preferred extractant, because it is a liquid at room temperature, while TOPO is a solid with a melting point of 52 °C, and would have to be dissolved in a suitable diluent or derivatized (e.g., as isoctyl compound) to become a liquid.

**ITC.** Figure 4a shows a result of a calorimetric titration of phenol with TOPO in dry toluene. The binding of phenol to

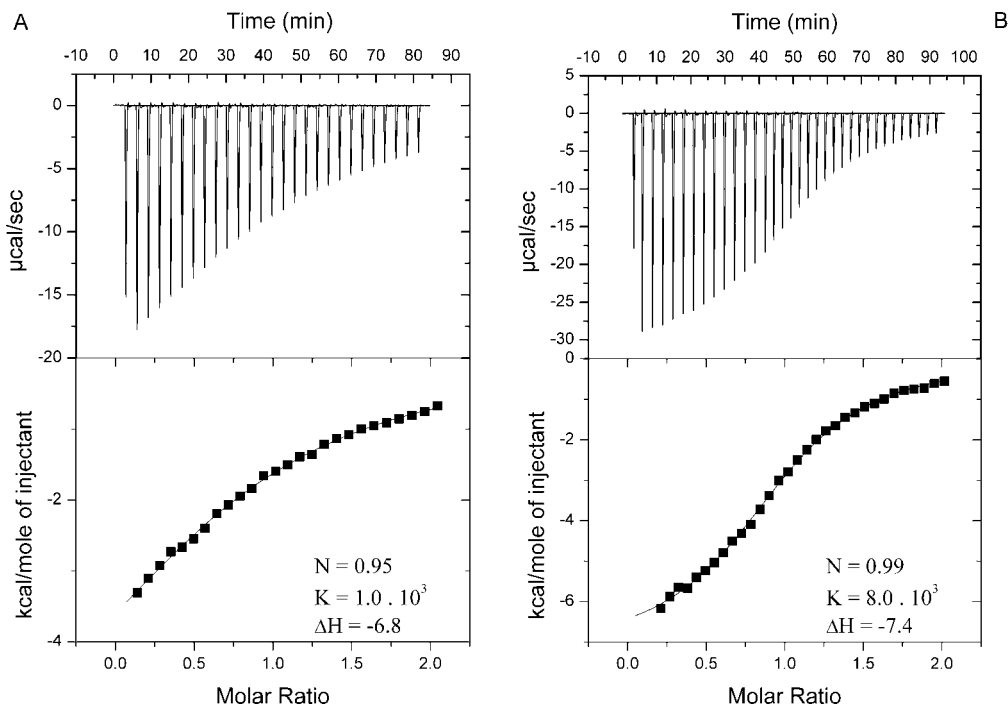


**Figure 4.** Binding isotherms for TOPO–phenol complexes at 30 °C. Top pane: raw data. Lower pane: processed binding isotherm. Syringe: TOPO in dry toluene (10.8 mM). Cell: (A) phenol (1.08 mM in dry toluene); (B) 4-cyanophenol (1.09 mM in dry toluene).

**TABLE 3: ITC Results Listing All Thermodynamic Parameters for TOPO–Phenol Complexes and the TBP–Phenol Complex<sup>a</sup>**

complex	<i>N</i>	<i>K</i>	$\Delta H$	$\Delta G$	$T\Delta S$
TOPO–phenol <sup>b</sup>	0.95 ± 0.01	(1.0 ± 0.1) × 10 <sup>3</sup>	−6.8 ± 0.2	−4.2 ± 0.1	−2.6 ± 0.1
TOPO–phenol <sup>c</sup>	1.07 ± 0.02	(5.8 ± 1.2) × 10 <sup>2</sup>	−6.9 ± 0.5	−3.8 ± 0.1	−3.0 ± 0.6
TOPO–3-chlorophenol <sup>b</sup>	0.97 ± 0.07	(3.5 ± 0.5) × 10 <sup>3</sup>	−7.1 ± 0.3	−4.9 ± 0.1	−2.2 ± 0.2
TOPO–3-chlorophenol <sup>c</sup>	1.11 ± 0.01	(1.6 ± 0.5) × 10 <sup>3</sup>	−9.2 ± 1.2	−4.4 ± 0.2	−4.8 ± 1.4
TOPO–3,5-dichlorophenol <sup>b</sup>	1.01 ± 0.05	(9.8 ± 0.4) × 10 <sup>3</sup>	−7.1 ± 0.1	−5.5 ± 0.0	−1.6 ± 0.1
TOPO–3,5-dichlorophenol <sup>c</sup>	1.16 ± 0.01	(4.0 ± 1.0) × 10 <sup>3</sup>	−8.6 ± 0.8	−5.0 ± 0.2	−3.6 ± 1.0
TOPO–4-cyanophenol <sup>b</sup>	0.99 ± 0.08	(8.0 ± 0.6) × 10 <sup>3</sup>	−7.4 ± 0.3	−5.4 ± 0.1	−2.0 ± 0.3
TOPO–4-cyanophenol <sup>c</sup>	1.09 ± 0.11	(5.4 ± 2.5) × 10 <sup>3</sup>	−8.1 ± 1.0	−5.1 ± 0.3	−3.0 ± 1.2
TOPO–pentachlorophenol <sup>b</sup>	0.88 ± 0.03	(1.1 ± 0.1) × 10 <sup>3</sup>	−8.7 ± 0.7	−4.2 ± 0.1	−4.5 ± 0.6
TOPO–pentachlorophenol <sup>c</sup>	0.94 ± 0.04	(7.7 ± 0.8) × 10 <sup>2</sup>	−8.6 ± 0.6	−4.0 ± 0.1	−4.6 ± 0.6
TBP–phenol <sup>b</sup>	0.98 ± 0.10	(9.2 ± 0.9) × 10 <sup>1</sup>	−5.8 ± 0.8	−2.7 ± 0.1	−3.0 ± 0.9
TBP–phenol <sup>c</sup>	1.01 ± 0.20	(5.9 ± 0.5) × 10 <sup>1</sup>	−8.1 ± 0.7	−2.5 ± 0.1	−5.7 ± 0.8

<sup>a</sup> Stoichiometry *N*, binding affinity *K* (M<sup>−1</sup>), enthalpy of complexation  $\Delta H$  (kcal/mol), change in Gibbs free energy  $\Delta G$  (kcal/mol), and the entropy  $T\Delta S$  (kcal/mol). <sup>b</sup> Solvent: dry toluene. <sup>c</sup> Solvent: water-saturated toluene.

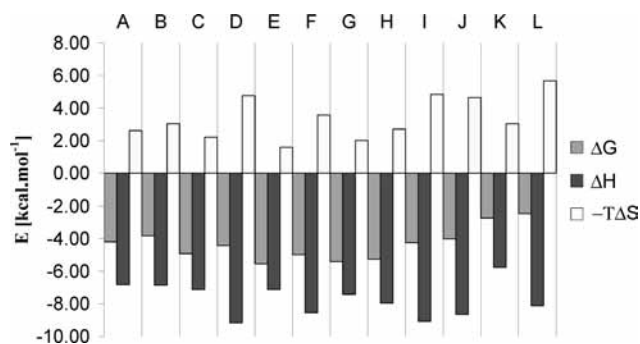
TOPO is exothermic, with  $\Delta H = -6.8$  kcal/mol and  $K_{\text{chem}} = 1.0 \times 10^3 \text{ M}^{-1}$ . The molar ratio of TOPO/phenol was 0.95 at saturation, indicating that there are no other effects that interfere with direct binding of phenol to TOPO, a fact that was also shown to be true for the other combinations. The entropy factor  $T\Delta S$  is negative, indicating an overall increased order upon binding. Apparently, the complexing agents either do not have strong interactions with the surrounding medium, or those interactions do not significantly change upon complexation. The values of all thermodynamic parameters obtained for the different complexes are listed in Table 3.

Figure 4b depicts the calorimetric titration of 4-cyanophenol with TOPO in dry toluene. In this case, a clearly sigmoid curve can be observed, which is indicative for strong binding of the solute to the complexing agent, as confirmed by the much higher binding affinity ( $K_{\text{chem}} = 8.0 \times 10^3 \text{ M}^{-1}$ ). The higher value is in line with the electron-withdrawing capacity of the 4-CN moiety, which makes this phenol more acidic and therefore a better hydrogen-bond donor.

The changes in  $\Delta G$  upon binding of the phenols with electron-withdrawing substituents (3-chlorophenol, 3,5-dichlorophenol,

and 4-cyanophenol with  $\text{p}K_{\text{a}}$  values of 9.02,<sup>75</sup> 8.04,<sup>76</sup> and 7.95,<sup>75</sup> respectively) are significantly higher than those for phenol itself, accordingly leading to much higher binding affinities for the former phenols. Again, the influence of  $T\Delta S$  to complex formation is negative, so that complexation is enthalpy driven. For pentachlorophenol ( $\text{p}K_{\text{a}} = 4.68$ <sup>76</sup>) the change in  $\Delta G$  is also higher than that for phenol itself (as expected from the very low  $\text{p}K_{\text{a}}$ ), but judging from the very large inhibiting effect of  $T\Delta S$ , solvent interactions prevent the formation of a very strong hydrogen bond. As a result,  $K_{\text{chem}}$  was found to be only marginally higher than for phenol ( $K_{\text{chem}} = 1.1 \times 10^3 \text{ M}^{-1}$  vs  $1.0 \times 10^3 \text{ M}^{-1}$  for phenol), in contrast to results in the literature,<sup>26,32</sup> where pentachlorophenol was found to have a lower binding affinity toward complexing agents with the P=O moiety (obtained from IR measurements in  $\text{CCl}_4$ ).

In the presence of water, the affinity of phenols toward TOPO is significantly lower. Binding affinities in the presence of water range from  $5.8 \times 10^2 \text{ M}^{-1}$  for phenol, which was in excellent agreement with the liquid–liquid experiments ( $579 \text{ M}^{-1}$ ; vide supra, Table 2), to  $5.4 \times 10^3 \text{ M}^{-1}$  for 4-cyanophenol. This amounts to a water-induced decrease in  $K_{\text{D}}$  of 30–60%. The



**Figure 5.** Energetic fingerprints of extractant–phenol complexes: (A) TOPO–phenol; (B) TOPO–phenol, water present; (C) TOPO–3-chlorophenol; (D) TOPO–3-chlorophenol, water present; (E) TOPO–3,5-dichlorophenol; (F) TOPO–3,5-dichlorophenol, water present; (G) TOPO–4-cyanophenol; (H) TOPO–4-cyanophenol, water present; (I) TOPO–pentachlorophenol; (J) TOPO–pentachlorophenol, water present; (K) TBP–phenol; (L) TBP–phenol, water present.

main reason for this decrease is the unfavorable change in entropy. For the TOPO–phenol complex, the differences are the smallest:  $\Delta H$  in the presence of water is only 1.5% more negative, whereas  $\Delta S$  is over 15% more negative. For the phenols with electron-withdrawing groups these differences are much larger:  $\Delta H$  is 9–30% more negative in the presence of water, whereas  $\Delta S$  is 50–125% more negative. Thus, hydrogen bond formation is found to be more favorable ( $\Delta H$  is more negative), as additional hydrogen bonds can be formed with the water molecules. However, complex formation is severely hindered by the large negative change in entropy ( $\Delta S$  is more negative), so that  $\Delta G$  is found to be less negative than in the water-free case. This indicates cocomplexation of water by the extractants, where the water molecules are bound tightly to the extractant–phenol complex, losing much of their entropic freedom. Water binding by TOPO in the absence of phenol has been the subject of investigation, but because of the very low heat effect this could not be quantified.

For TOPO–pentachlorophenol complexes, the influence of the water is different. In line with previous results, the binding affinity in the presence of water is significantly lower (by 32%). However,  $\Delta H$  is less negative in the presence of water and  $\Delta S$  is hardly affected by the water, in contrast to the other TOPO–phenol complexes. Presumably, the five chlorine atoms show some favorable interaction with the water environment. This means that although in principle much stronger hydrogen bonds could be formed between TOPO and pentachlorophenol in comparison to phenol, this effect is nearly eliminated by the large unfavorable change in entropy, due to the loss of entropic freedom of the water molecules in the vicinity of the complex.

The “energetic signatures”, in which the thermodynamic parameters of the investigated interactions are compared graphically, are given in Figure 5. In general, there are three different types of energetic signatures:<sup>38</sup> one for favorable interaction due to hydrogen bond formation, one for van der Waals interactions, and one for a combined process. In hydrogen bond formation, the signature is characterized by a high negative value of  $\Delta H$ , and a relatively small negative value for  $T\Delta S$ . This is completely in line with the results obtained here. All TOPO–phenol interactions discussed here show the same signature, which is thus indicative for hydrogen bond formation accompanied by a loss of entropic freedom.<sup>38</sup> This effect is more pronounced in the cases where there is water present, as has just been discussed.

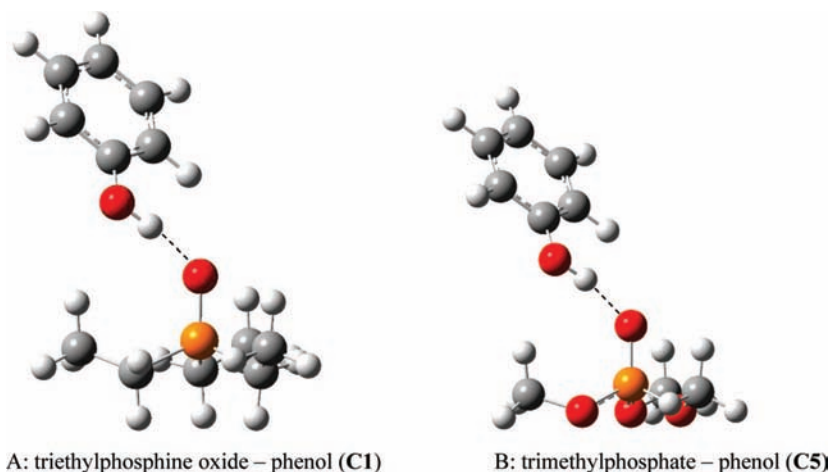
In addition to these experiments, ITC measurements have also been performed on the tributylphosphate (TBP)–phenol, tri-

isobutylphosphine sulfide (TIBPS)–phenol, and TOPO–thiophenol complexes. The thermodynamic parameters for the TBP–phenol interactions are given in Table 3. The heat effects measured upon TIBPS–phenol and TOPO–thiophenol interaction were both very low, even at high concentrations. Since the experimental errors in those measurements were therefore relatively large, it was not possible to calculate accurate quantitative thermodynamic parameters from these measurements, both in the absence and in the presence of water. The binding affinities  $K_{\text{chem}}$  for the TIBPS–phenol and TOPO–thiophenol interactions in the absence of water were found to be approximately 8 and 85  $\text{M}^{-1}$ , respectively, indicating that hydrogen bonds via sulfur atoms are indeed much weaker than the corresponding  $\text{O}-\text{H}\cdots\text{O}$  hydrogen bonds present in, e.g., the TOPO–phenol complex ( $K_{\text{chem}} = 1.0 \times 10^3 \text{ M}^{-1}$ ).

The TBP binding to phenol ( $K_{\text{chem}} = 92 \text{ M}^{-1}$ ) indicates that phosphate–phenol binding is indeed much weaker than phosphine oxide–phenol binding, as was also found with liquid–liquid extraction experiments. The phosphate–phenol complexes were formed in a 1:1 ratio, as was also found for the phosphine oxides. While  $\Delta G$  is negative, there is clearly less driving force available than for the formation of the phosphine oxide–phenol complex, largely caused by a reduced enthalpy change. However, in the presence of water, a much larger change of  $\Delta H$  was found, which is indicative for cocomplexation of water molecules to the TBP. This was again accompanied by a much larger negative entropy change upon complexation, due to the loss of entropy for the water molecules upon binding to TBP.

**DFT and MP2 Computations.** In the following section, first phosphine oxide–phenol complexes will be discussed, subsequently the phosphate–phenol complexes, and finally substituent effects on the phosphine oxide–substituted phenol complexes.

**Phosphine Oxides–Phenol Complexes.** As can be seen from the optimized geometries of the selected phosphine oxide–phenol and phosphate–phenol complexes (Figure 6a,b and the Supporting Information), phenols form a hydrogen bond to the  $\text{P}=\text{O}$  moiety, showing a geometry with a near-ideal linear hydrogen bond. In the triethylphosphine oxide (TEPO)–phenol complex (complex C1, Figure 6a), the hydrogen bond length is short ( $d = 1.72 \text{ \AA}$ ) and the hydrogen bond angle is almost perfectly linear ( $\alpha = 171^\circ$ , Table 4). In addition, the bond lengthening of the hydrogen bond donor is substantial ( $\Delta r = 0.021 \text{ \AA}$ ) and the dihedral angle of the phenol is close to zero ( $\phi = -2.2^\circ$ ). The enthalpy of complexation  $\Delta H$  (in vacuum) in complex C1 is found to be  $-12.0 \text{ kcal/mol}$  at the B3LYP and MP2 levels of theory, whereas  $\Delta H$  in toluene (B3LYP) was  $-10.7 \text{ kcal/mol}$ . With respect to the B3LYP values, the calculated MP2 values for the enthalpy of complex formation for phosphine oxide–phenol complexes are typically equal or slightly more negative, in line with trends from the literature.<sup>51</sup> Results show that complex formation in toluene is slightly less favorable than in vacuum, by  $\sim 1.3 \text{ kcal/mol}$ . This indicates a minor solvent effect, as was also clear from the solvation energies of the solutes and complexes. The natural population analysis (NPA) charges on the oxygen of the phosphine oxide and the hydrogen of the phenol alcohol moiety were found to be  $-1.11$  and  $+0.51$  (see Table 4), respectively, which points to a strong electrostatic tendency for hydrogen bonding. Some covalent character is also apparent, as can be deduced from the atom–atom overlap-weighted NAO bond orders. For example, the bond order between the TEPO oxygen and the phenol hydrogen amounts to 0.076, while the bond order in the phenol  $\text{O}-\text{H}$  bond was found to be 0.600, i.e. 0.061 smaller than that in the isolated phenol molecule (cf. Supporting Information).



A: triethylphosphine oxide – phenol (C1)

B: trimethylphosphate – phenol (C5)

**Figure 6.** Optimized structures (B3LYP/6-311G(d,p) (vacuum)) of representative phosphine oxide–phenol and phosphate–phenol complexes. Orange: phosphorus; red: oxygen; black: carbon; white: hydrogen.

**TABLE 4: Selected Geometric Parameters (see Table 1), Enthalpy of Complexation  $\Delta H$  (kcal/mol), and Charges on Hydrogen Bond Forming Atoms of the Triethylphosphine Oxide (TEPO) and Triethylphosphine Sulfide (TEPS) Complexes with Phenol and Thiophenol<sup>a</sup>**

no.	complex	geometric parameters				$\Delta H$			NPA charge (B3LYP)	
		$d$	$\alpha$	$\Delta r^b$	$\phi$	$\Delta H$		phosphine O or S	phenol H	
						B3LYP	MP2			
						vacuum	toluene	vacuum		
C1	TEPO–phenol	1.72	171	0.021	–2.2	–12.0	–10.7	–12.0	–1.11	+0.51
C2	TEPO–thiophenol	2.00	172	0.011	–5.3	–6.5	–5.4	–7.6	–1.09	+0.19
C3	TEPS–phenol	2.36	171	0.012	+3.4	–6.3	–5.1	–9.4	–0.66	+0.49
C4	TEPS–thiophenol	2.63	170	0.010	–9.4	–3.7	–2.9	–6.5	–0.64	+0.16

<sup>a</sup>  $d$ ,  $\alpha$ ,  $\Delta r$ , and  $\phi$ , as shown in Table 1. <sup>b</sup>  $\Delta r = d(\text{O–H})$  in the complex –  $d(\text{O–H})$  of noncomplexed phenol; analogous for S ( $d(\text{O–H})_{\text{phenol}} = 0.963 \text{ \AA}$ ;  $d(\text{S–H})_{\text{thiophenol}} = 1.347 \text{ \AA}$ ).

These theoretical findings suggest that a strong hydrogen bond is formed in a 1:1 ratio of phosphine oxide and phenol. This is supported by the liquid–liquid extraction (high distribution coefficients  $K_D$ ) and ITC results (high  $K_{\text{chem}}$ , high negative  $\Delta H$  and  $\Delta G$ , and  $N = 0.95$ – $0.99$ ). The modeling data predict a more negative  $\Delta H$  than obtained with the ITC, i.e., for the TOPO–phenol complex  $\Delta H_{\text{ITC}} = -6.8 \text{ kcal/mol}$  (Table 3), while  $\Delta H_{\text{theo}}^{\text{phenol}} = -10.7 \text{ kcal/mol}$  (Table 4). Since B3LYP and MP2 yield highly similar data, two factors may seem to attribute this quantitative gap: an incomplete description of the solvent effects by the PCM model, and a contribution of less-than-optimal geometries in the experimental situation, caused by the dynamic nature of hydrogen bond formation. As the theoretical description of solvent effects will likely continue to improve, a more detailed dissection can be expected in the future.

By comparing the overall distribution coefficient  $K_D$  and the physical and chemical distribution coefficients  $K_{\text{phys}}$  and  $K_{\text{chem}}$  of phenol for a TOPO solution in toluene, it can be seen that the main source for the overall distribution coefficient of  $\sim 580$  is the binding of phenol to phosphine oxide with a high binding affinity  $K_{\text{chem}}$ . This clearly shows that reactive extraction can indeed increase the effective partitioning of phenols into the extraction liquid by several orders of magnitude!

The TEPO–thiophenol complex (complex C2) shows much lower binding enthalpy values, as was also observed in the ITC measurements. The charge on the thiophenol hydrogen is much smaller than that for the phenol hydrogen in the corresponding TEPO–phenol complex discussed before, which is the main source for the negative influence of the sulfur atom on the hydrogen bonding. Also the bond order of the hydrogen bond is found to be much lower than that for the TEPO–phenol complex (0.038 vs 0.076 for TEPO–phenol, vide supra).

The phosphine sulfide complexes to phenol and thiophenol (complexes C3 and C4) both show even less negative enthalpies of complexation; the least negative were found for the triethylphosphine sulfide (TEPS)–thiophenol complex. The clearest geometrical differences come from the lengthening of the involved O–H and S–H bonds, which were clearly smaller when sulfur was involved ( $\Delta r = 0.010$ – $0.012 \text{ \AA}$  for complexes with sulfur;  $\Delta r = 0.021 \text{ \AA}$  for TEPO–phenol). In line with this, the NPA charges on the sulfur atom of the phosphine sulfide are found to be much less negative than on the corresponding oxygen atom of the phosphine oxide. Again, the sulfur atom is the cause for the reduced tendency to form complexes. Also the lower bond orders of the atoms in the hydrogen bond reflect this weaker binding; the NAO  $\text{O}\cdots\text{H}$  bond order amounts to 0.047 and 0.045 for TEPS–phenol and TEPS–thiophenol, respectively.

The dihedral angles of the O–H or S–H bonds of the phenols with respect to their benzene ring are found to be close to the ideal value of  $0^\circ$ . However, some small differences between phenols and thiophenols can be seen. Hydrogen-bound thiophenols tend to show a somewhat larger dihedral angle than phenols. These differences can be understood from the energy barriers of the rotation around the C–O/C–S bond. For phenol, the energy barriers ( $E_{\text{O–H}} \text{ at } 90^\circ - E_{\text{O–H}} \text{ at } 0^\circ$ , angle with respect to the plane of the benzene ring) are calculated to be 3.5 and 3.0 kcal/mol (B3LYP and MP2, respectively), while for thiophenol, the corresponding values are calculated to be only 0.7 and 0.4 kcal/mol, respectively.

**Phosphate–Phenol Complexes.** As can be seen from Figure 6b, phenol forms a similar hydrogen bond to trimethylphosphate (TMP) as to triethylphosphine oxide (TEPO). As expected, within the class of phosphates and thiophosphates the TMP–



**TABLE 5: Selected Geometric Parameters (see Table 1), Enthalpy of Complexation  $\Delta H$  (kcal/mol), and Charges on Hydrogen Bond Forming atoms of the Trimethylphosphate (TMP) and Trimethylthiophosphate (TMTP) Complexes with Phenol and Thiophenol<sup>a</sup>**

no.	complex	geometric parameters				$\Delta H$				
						B3LYP		MP2	NPA charge (B3LYP)	
		$d$	$\alpha$	$\Delta r^b$	$\phi$	vacuum	toluene	vacuum	phosphine O or S	phenol H
<b>C5</b>	TMP–phenol	1.76	168	0.016	–1.4	–9.8	–8.3	–9.8	–1.11	+0.52
<b>C6</b>	TMP–thiophenol	2.06	169	0.008	–7.3	–5.0	–4.0	–6.3	–1.10	+0.18
<b>C7</b>	TMTP–phenol	2.43	167	0.009	+4.5	–4.8	–3.5	–6.0	–0.66	+0.49
<b>C8</b>	TMTP–thiophenol	2.78	171	0.004	–16.6	–2.4	–1.6	–4.6	–0.63	+0.15

<sup>a</sup>  $d$ ,  $\alpha$ ,  $\Delta r$ , and  $\phi$ , as shown in Table 1. <sup>b</sup>  $\Delta r = d(\text{O–H})$  in the complex –  $d(\text{O–H})$  of noncomplexed phenol; analogous for S ( $d(\text{O–H})_{\text{phenol}} = 0.963 \text{ \AA}$ ;  $d(\text{S–H})_{\text{thiophenol}} = 1.347 \text{ \AA}$ ).

**TABLE 6: Selected Geometric Parameters (see Table 1) and Enthalpy of Complexation  $\Delta H$  (kcal/mol) of the TEPO Complexes with Substituted Phenols<sup>a</sup>**

no.	complex	geometric parameters				$\Delta H$		
						B3LYP		MP2
		$d$	$\alpha$	$\Delta r^b$	$\phi$	vacuum	toluene	vacuum
<b>C9</b>	TEPO–3-Cl-PhOH	1.69	173	0.024	–2.0	–13.5	–12.1	–13.3
<b>C10</b>	TEPO–3,5-Cl <sub>2</sub> -PhOH	1.66	174	0.026	–2.8	–14.7	–13.2	–14.4
<b>C11</b>	TEPO–4-CN-PhOH	1.67	173	0.027	–3.2	–14.9	–13.4	–14.3
<b>C12</b>	TEPO–Cl <sub>5</sub> -PhOH	1.66	155	0.031	4.2	–11.8	–10.5	–11.5

<sup>a</sup>  $d$ ,  $\alpha$ ,  $\Delta r$ , and  $\phi$ , as shown in Table 1. <sup>b</sup>  $\Delta r = d(\text{O–H})$  in the complex –  $d(\text{O–H})$  of the phenol molecule ( $d(\text{O–H})_{\text{phenol}} = 0.963 \text{ \AA}$  in all cases).

phenol complexes show the highest complexing enthalpies (Table 5). These results are supported by the fact that hydrogen bond lengths are found to be shortest for TMP–phenol complexes and much longer for the complexes involving sulfur atoms, and they reflect the much higher tendency of oxygen over sulfur to form strong hydrogen bonds. With respect to the dihedral angle  $\phi$  of phenol and thiophenol it was found that especially the thiophenol complexes again show a tendency to twist the thiol group out of plane of the benzene ring.

From Table 5 it can be seen that for thiophenol, charges on the relevant atoms are much smaller in absolute numbers than for phenol. The charge on the phenolic hydrogen atom is ca. +0.5, whereas the charge on the corresponding thiophenol hydrogen atom is ca. +0.2, in line with the observation that hydrogen bonds by thiophenol are intrinsically much weaker than those formed by phenol. The difference between phosphate and thiophosphate can also be clearly observed. The charges on the phosphate oxygen atom and sulfur atom are around –1.1 and –0.6, respectively. This means that the thiophosphate compounds will form weaker hydrogen bonds, in line with both our experimental and theoretical results for the tendency for complexation.

The bond order of the TMP–phenol hydrogen bond was found to be 0.063, a somewhat lower value than what was found for TEPO–phenol (0.076). The bond orders of the hydrogen bonds that involve one or two sulfur atoms were found to be significantly smaller: 0.034 (TMP–thiophenol), 0.032 (TMTP–phenol), and 0.021 (TMTP–thiophenol).

No significant differences in the charges of the directly involved atoms have been found between phosphine oxides and phosphates. However, the fact that phosphates and thiophosphates form weaker complexes than their respective phosphine oxides and sulfides is consistently reflected in differences in orbital overlap, as indicated above. An additional calculation result is that the hydrogen bond length  $d$  for the complexes of phosphine oxides and sulfides is consistently smaller than that for the corresponding complexes of the phosphates and thiophosphates (cf. values of  $d$  in Table 4 versus Table 5).

On the basis of the calculated enthalpies of complex formation, the most suitable extractant for both phenol and thiophenol extraction in the series investigated here is triethylphosphine oxide, as it yields the most negative  $\Delta H$  upon complex formation. In addition, the liquid–liquid extraction experiments also point to the phosphine oxides as optimal extractants.

**Triethylphosphine Oxide (TEPO)–Substituted Phenol Complexes.** From Table 6 it can be seen that binding enthalpies of as much as 14.4 kcal/mol (for 4-cyanophenol, MP2, vacuum) are found for TEPO–substituted phenol complexes with electron-withdrawing substituents on the phenol. These values are more negative than the value of –12.0 kcal/mol found for the TEPO–phenol complex (complex **C1**, vide supra). This points to a positive influence of electron-withdrawing moieties attached to the phenolic compounds on the acidity of the O–H group, and therefore on the binding affinity  $K_{\text{chem}}$ . For the TEPO–pentachlorophenol complex a  $\Delta H$  value of –11.5 kcal/mol was found, slightly less negative than that for the TEPO–phenol complex. Apparently, the pentachlorophenol does not yield additional hydrogen-bonding energy, but loses some. This effect might be due to the chlorine atoms, which force the TEPO–pentachlorophenol complex into a slightly different geometry thereby diverting it from the hydrogen bond optimal geometry. This effect can also be seen in the slightly deviating bond angle ( $\alpha = 155^\circ$ ).

Also in the geometric parameters the superior strength of these substituted phenol complexes can be seen. Relatively short hydrogen bonds ( $d$  ranges from 1.66 to 1.69 Å) and a significant lengthening of the O–H bond length ( $\Delta r$  ranges from 0.024 to 0.031 Å) are found, indicative of strong hydrogen bonds. The hydrogen bond angles are very close to the ideal value of  $180^\circ$ , except for the pentachlorophenol complex for reasons just discussed. Charges on all four complexes were found to be very similar. On the TEPO oxygen atom, the charge was –1.14, slightly higher than that for the TEPO–phenol complex (–1.10). The charge on the phenol hydrogen was found to be +0.52 for the substituted phenols, near-identical to the value found for phenol itself. Atom–atom overlap-weighted NAO bond orders



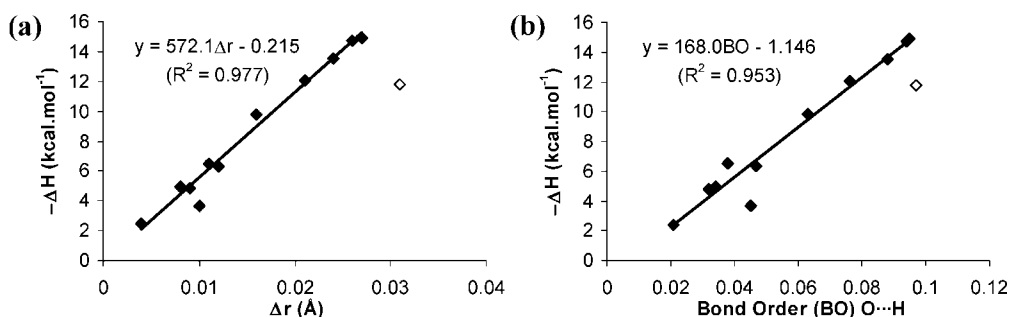


**Figure 7.** Dependence of binding enthalpy  $-\Delta H$  on O–H bond lengthening  $\Delta r$  (a) and on the O...H NAO bond order (b). The TEPO–pentachlorophenol data (open symbols) are indicated but not included in the trend lines (B3LYP data, in vacuo).

for the hydrogen bond in these TEPO–substituted phenol complexes range from 0.088 to 0.097. These are significantly higher than that for the TEPO–phenol complex (0.076), which suggests that orbital overlap plays a significant role in determining the substituent effects on the stability of the hydrogen-bonded complexes. An interesting feature of the TEPO–pentachlorophenol complex is the much lower NAO bond order between the phenol oxygen and phenol hydrogen, in comparison to the other substituted phenol complexes (see the Supporting Information). This indicates that in this case, although governed by O...H orbital overlap, the complex formation is also influenced by a decrease of O–H orbital overlap in the pentachlorophenol itself, thereby weakening the complex substantially. Presumably, the abundance of electronegative chlorine atoms stabilizes the partly bound phenolate species. This can also be an explanation for the deviating hydrogen bond angle that was found for the TEPO–pentachlorophenol complex.

An interesting phenomenon can be observed if the enthalpy data  $\Delta H$  are plotted against the bond lengthening  $\Delta r$  for the calculated complexes (Figure 7a). The lengthening of the O–H bond ( $\Delta r$ ) increases proportionally with increasing complexation enthalpy (except for pentachlorophenol, for reasons discussed above). Also the NPA bond order is linearly correlated to the complexation enthalpy (Figure 7b; except for pentachlorophenol, for reasons discussed above). This indicates that the amount of orbital overlap between the hydrogen bond donor and acceptor is directly linked to the energy gain on complex formation. These results of strong hydrogen bonds of TEPO to substituted phenols are supported by the findings in the ITC experiments, where it was shown that all four phenols with electron-withdrawing groups (i.e., higher acidities) yield higher binding affinities toward TOPO than phenol.

## Conclusions

The combination of liquid–liquid extraction and isothermal calorimetry experiments together with ab initio molecular modeling provides a detailed view of the interaction between phenols and phosphates and between phenols and phosphine oxides. The obtained data indicate that the binding of the extractants increases in the order trialkylphosphine sulfide  $\ll$  phosphate < phosphine oxide. Distribution coefficients  $K_D$  for phenol, ranging from 6 for triisobutylphosphine sulfide to  $\sim 880$  for the phosphine oxides, are largely the effect of hydrogen bond formation with equilibrium constant  $K_{\text{chem}}$ .

The ITC experiments showed that the phenol–phosphine oxide interaction is primarily due to hydrogen bonding. The interaction of substituted phenols with trioctylphosphine oxide clearly increases in the order phenol < pentachlorophenol < 3-chlorophenol < 4-cyanophenol  $\approx$  3,5-dichlorophenol (in line with their  $pK_a$  values, except for pentachlorophenol), with

binding constants from  $1.0 \times 10^3 \text{ M}^{-1}$  for phenol to  $9.8 \times 10^3 \text{ M}^{-1}$  for 3,5-dichlorophenol in the absence of water. In the presence of water, binding affinities are lowered by 30–60%, due to cocomplexation of water.

Modeling results indeed confirm that the interaction takes place via hydrogen bond formation. The binding strength is found to be high for the phosphine oxide–phenol/phosphate–phenol complexes, and much lower if thio-compounds are involved. This negative influence of sulfur is clearly related to the much smaller negative charges on S (in comparison to O), which yields smaller electrostatic interactions, smaller atom–atom overlap-weighted NAO bond orders, and correspondingly weaker hydrogen bonds. NAO bond orders are found to directly influence the hydrogen bond strength. The binding affinity  $K_{\text{chem}}$  is found to increase substantially by the introduction of electron-withdrawing substituents on the phenols, in line with their respective  $pK_a$  values.

A deviation is found for the complexes with pentachlorophenol. Although complexing of pentachlorophenol is stronger than that of phenol, the  $T\Delta S$  factor shows that the presence of water affects complexation in an inhibiting way. Computations show that complexation is still governed by hydrogen bond formation, but the bound complex is destabilized by the presence of the electronegative chlorine atoms, leading to lower binding enthalpies.

Finally, the choice of the optimum extractant is crucial for future SIR applications. The combination of extraction, ITC, and modeling experiments shows that phosphine oxides are good candidates for the extraction of phenols from aqueous media. In combination with industrially relevant properties such as a low melting point (removes the need for additional diluent) and a high boiling point (for regeneration of the SIR at high temperatures), it becomes clear that the phosphine oxide blend Cyanex 923 combines many of these desired characteristics.

**Acknowledgment.** The authors kindly acknowledge André ten Böhmer for technical assistance and the Technology Foundation STW for financial support of project 06347.

**Supporting Information Available:** Geometries of the calculated complexes and energy values and bond orders for individual molecules and complexes. This material is available free of charge via the Internet at <http://pubs.acs.org>.

## References and Notes

- (1) Cortina, J. L.; Warshawsky, A. *Developments in Solid-Liquid Extraction by Solvent-Impregnated Resins*. In *Ion Exchange Solvent Extraction*; Marinsky, J. A., Marcus, Y., Eds.; Dekker: New York, 1997; Vol. 13; p 195.
- (2) Ohnaka, K.; Yuchi, A. *Chem. Lett.* **2005**, *34*, 868.

- (3) Saha, B.; Gill, R. J.; Bailey, D. G.; Kabay, N.; Arda, M. *React. Funct. Polym.* **2004**, *60*, 223.
- (4) Draa, M. T.; Belaid, T.; Benamor, M. *Sep. Purif. Technol.* **2004**, *40*, 77.
- (5) Alexandratos, S. D.; Smith, S. D. *Solvent Extr. Ion Exch.* **2004**, *22*, 713.
- (6) Wang, Y.; Wang, C.; Warshawsky, A.; Berkowitz, B. *Sep. Sci. Technol.* **2003**, *38*, 149.
- (7) Gupta, B. B.; Ismail, Z. B. *Compos. Interfaces* **2006**, *13*, 487.
- (8) El-Dessouky, S. S.; Borai, E. H. *J. Radioanal. Nucl. Chem.* **2006**, *268*, 247.
- (9) Liu, J. S.; Chen, H.; Guo, Z. L.; Hu, Y. C. *J. Appl. Polym. Sci.* **2006**, *100*, 253.
- (10) Serarols, J.; Poch, J.; Villaescusa, I. *React. Funct. Polym.* **2001**, *48*, 37.
- (11) Warshawsky, A.; Cortina, J. L.; Aguilar, M.; Jerabek, K. New Developments in Solvent Impregnated Resins. An Overview; International Solvent Extraction Conference, Barcelona, Spain, 1999.
- (12) *Membrane Technology* **2007**, September 4.
- (13) Juang, R.-S.; Chang, H.-L. *Ind. Eng. Chem. Res.* **1995**, *34*, 1294.
- (14) Traving, M.; Bart, H.-J. *Chem. Eng. Technol.* **2002**, *25*, 997.
- (15) Kostova, A.; Bart, H.-J. *Chem. Ing. Tech.* **2004**, *76*, 1743.
- (16) Kitazaki, H.; Ishimaru, M.; Inoue, K.; Yoshida, K.; Nakamura, S. Separation and Recovery of Flavonoids by means of Solvent Extraction and Adsorption on Solvent-Impregnated Resin; International Solvent Extraction Conference, Melbourne, Australia, 1996.
- (17) Babic, K.; Driessen, G. H. M.; van der Ham, A. G. J.; de Haan, A. B. *J. Chromatogr. A* **2007**, *1142*, 84.
- (18) Other important factors are the total extractant concentration in the resin (low concentration, high concentration, or possibly pure), and the nature of the solvent (good or bad solvent for solute and extractant, low solvent leakage). Optimization of these factors is desirable to make the process material- and cost-effective.
- (19) Lazarova, Z.; Boyadzhieva, S. *Chem. Eng. J.* **2004**, *100*, 129.
- (20) Cichy, W. W.; Szymanowski, J. *J. Environ. Sci. Technol.* **2002**, *36*, 2088.
- (21) Earhart, J. P.; Won, K. W.; Wong, H. Y.; Prausnitz, J. M.; King, C. *J. Chem. Eng. Prog.* **1977**, *73*, 67.
- (22) Jeffrey, G. A. *An Introduction to Hydrogen Bonding*; Oxford University Press: New York, 1997, and references cited therein.
- (23) Johnson, E. R.; McKay, D. J. J.; DiLabio, G. A. *Chem. Phys. Lett.* **2007**, *435*, 201.
- (24) Lommerse, J. P. M.; Price, S. L.; Taylor, R. *J. Comput. Chem.* **1997**, *18*, 757.
- (25) Sunil, K.; Panigrahi, G. R. D. *Proteins: Structure, Function, Bioinformatics* **2007**, *67*, 128.
- (26) Abraham, M. H.; Grellier, P. L.; Prior, D. V.; Duce, P. P.; Morris, J. J.; Taylor, P. J. *J. Chem. Soc., Perkin Trans. 2* **1989**, 699.
- (27) Abraham, M. H.; Grellier, P. L.; Prior, D. V.; Morris, J. J.; Taylor, P. J. *J. Chem. Soc., Perkin Trans. 2* **1990**, 521.
- (28) Aksnes, G.; Albrigtsen, P. *Acta Chem. Scand.* **1968**, *22*, 1866.
- (29) Badger, R. M.; Bauer, S. H. *J. Chem. Phys.* **1937**, *5*, 839.
- (30) Fletcher, A. *J. Phys. Chem.* **1967**, *71*, 3742.
- (31) Fletcher, A. *J. Phys. Chem.* **1968**, *72*, 1839.
- (32) Gramstad, T. *Acta Chem. Scand.* **1961**, *15*, 1337.
- (33) Joesten, M. D.; Schaad, L. J. *Hydrogen Bonding*; Marcel Dekker: New York, 1974.
- (34) Leavitt, S.; Freire, E. *Curr. Opin. Struct. Biol.* **2001**, *11*, 560.
- (35) Wiseman, T.; Williston, S.; Brandts, J. F.; Lin, L.-N. *Anal. Biochem.* **1989**, *179*, 131.
- (36) Weber, P. C.; Salemme, F. R. *Curr. Opin. Struct. Biol.* **2003**, *13*, 115.
- (37) Ladbury, J. E. *Biotechniques* **2004**, *37*, 885.
- (38) Ladbury, J. E.; Doyle, M. L. *Biocalorimetry 2*; John Wiley & Sons, Ltd: New York, 2004.
- (39) Wiggers, H. J.; Cheliski, J.; Zottis, A.; Oliva, G.; Andricopulo, A. D.; Montanari, C. A. *Anal. Biochem.* **2007**, *370*, 107.
- (40) Ballester, P.; Capo, M.; Costa, A.; Deya, P. M.; Gomila, R.; Decken, A.; Deslongchamps, G. *J. Org. Chem.* **2002**, *67*, 8832.
- (41) Arnaud, A.; Bouteiller, L. *Langmuir* **2004**, *20*, 6858.
- (42) Merino-Garcia, D.; Andersen, S. I. *Langmuir* **2004**, *20*, 4559.
- (43) Merino-Garcia, D.; Andersen, S. I. *Pet. Sci. Technol.* **2003**, *21*, 507.
- (44) Sessler, J. L.; Gross, D. E.; Cho, W. S.; Lynch, V. M.; Schmidtchen, F. P.; Bates, G. W.; Light, M. E.; Gale, P. A. *J. Am. Chem. Soc.* **2006**, *128*, 12281.
- (45) Arnaud, A.; Bouteiller, L. *Langmuir* **2004**, *20*, 6858.
- (46) Xiang, M.; Jiang, M.; Zhang, Y.; Wu, C.; Feng, L. *Macromolecules* **1997**, *30*, 2313.
- (47) Mizutani, T.; Takagi, H.; Ueno, Y.; Horiguchi, T.; Yamamura, K.; Ogoshi, H. *J. Phys. Org. Chem.* **1998**, *11*, 737.
- (48) Johnson, E. R.; Clarkin, O. J.; DiLabio, G. A. *J. Phys. Chem. A* **2003**, *107*, 9953.
- (49) Jurečka, P.; Šponer, J.; Černý, J.; Hobza, P. *Phys. Chem. Chem. Phys.* **2006**, *8*, 1985.
- (50) Kryachko, E. S.; Nguyen, M. T. *J. Phys. Chem. A* **2002**, *106*, 4267.
- (51) Bienko, A. J.; Latajka, Z. *Chem. Phys. Lett.* **2003**, *374*, 577.
- (52) Kone, M.; Illien, B.; Graton, J.; Laurence, C. *J. Phys. Chem. A* **2005**, *109*, 11907.
- (53) Lopes, K. C.; Araujo, R. C.; M, U.; Rusu, V. H.; Ramos, M. N. *J. Mol. Struct.* **2007**, *834–836*, 258.
- (54) Zhao, Y.; Truhlar, D. G. *J. Chem. Theory Comput.* **2007**, *3*, 289.
- (55) Englin, B. A.; Platé, A. F.; Tugolukov, V. M.; Pryanishnikova, M. A. *Chem. Technol. Fuels Oils* **1965**, *1*, 722.
- (56) Chen, H.; Wagner, J. *J. Chem. Eng. Data* **1994**, *39*, 475.
- (57) Marche, C.; Ferronato, C.; DeHemptinne, J. C.; Jose, J. *J. Chem. Eng. Data* **2006**, *51*, 355.
- (58) Emerson, E. *J. Org. Chem.* **1943**, *8*, 417.
- (59) Ettinger, M.; Ruchhoff, C.; Lishka, R. *Anal. Chem.* **1951**, *23*, 1783.
- (60) Chellani, M. *Am. Biotechnol. Lab.* 1999, October 14.
- (61) Frisch, M. J.; Trucks, G. W.; Schlegel, H. B.; Scuseria, G. E.; Robb, M. A.; Cheeseman, J. R.; Montgomery, J. A., Jr.; Vreven, T.; Kudin, K. N.; Burant, J. C.; Millam, J. M.; Iyengar, S. S.; Tomasi, J.; Barone, V.; Mennucci, B.; Cossi, M.; Scalmani, G.; Rega, N.; Petersson, G. A.; Nakatsuji, H.; Hada, M.; Ehara, M.; Toyota, K.; Fukuda, R.; Hasegawa, J.; Ishida, M.; Nakajima, T.; Honda, Y.; Kitao, O.; Nakai, H.; Klene, M.; Li, X.; Knox, J. E.; Hratchian, H. P.; Cross, J. B.; Adamo, C.; Jaramillo, J.; Gomperts, R.; Stratmann, R. E.; Yazyev, O.; Austin, A. J.; Cammi, R.; Pomelli, C.; Ochterski, J. W.; Ayala, P. Y.; Morokuma, K.; Voth, G. A.; Salvador, P.; Dannenberg, J. J.; Zakrzewski, V. G.; Dapprich, S.; Daniels, A. D.; Strain, M. C.; Farkas, O.; Malick, D. K.; Rabuck, A. D.; Raghavachari, K.; Foresman, J. B.; Ortiz, J. V.; Cui, Q.; Baboul, A. G.; Clifford, S.; Cioslowski, J.; Stefanov, B. B.; Liu, G.; Liashenko, A.; Piskorz, P.; Komaromi, I.; Martin, R. L.; Fox, D. J.; Keith, T.; Al-Laham, M. A.; Peng, C. Y.; Nanayakkara, A.; Challacombe, M.; Gill, P. M. W.; Johnson, B.; Chen, W.; Wong, M. W.; Gonzalez, C.; Pople, J. A. *Gaussian 03, Revision C.02*; Gaussian, Inc.: Wallingford, CT, 2004.
- (62) Li, A. Y.; Wang, S. W. *J. Mol. Struct.: THEOCHEM* **2007**, *807*, 191.
- (63) Cramer, C. J. *Essentials Of Computational Chemistry: Theories And Models*, 2nd ed.; John Wiley & Sons, Ltd: New York, 2004.
- (64) Shchavlev, A. E.; Pankratov, A. N.; Shalabay, A. V. *Int. J. Quantum Chem.* **2006**, *106*, 876.
- (65) Lighthart, G. B. W. L.; Guo, D.; Spek, A. L.; Kooijman, H.; Zuilhof, H.; Sijbesma, R. P. *J. Org. Chem.* **2008**, *73*, 111.
- (66) Hadži, D. *Theoretical Treatments of Hydrogen Bonding*; John Wiley & Sons, Ltd: New York, 1997.
- (67) Umeyama, H.; Morokuma, K. *J. Am. Chem. Soc.* **1977**, *99*, 1316.
- (68) Cybulski, S.; Scheiner, S. *J. Phys. Chem.* **1990**, *94*, 6106.
- (69) Alagona, G. *Int. J. Quantum Chem.* **1987**, *32*, 227.
- (70) Reed, A. E.; Weinstock, R. B.; Weinhold, F. *J. Chem. Phys.* **1985**, *83*, 735.
- (71) Glendening, E. D.; Reed, A. E.; Carpenter, J. E.; Weinhold, F., NBO Version 3.1.
- (72) Liu, B.; McLean, A. D. *J. Chem. Phys.* **1973**, *59*, 4557.
- (73) Boys, S. F.; Bernardi, F. *Mol. Phys.* **1970**, *19*, 553.
- (74) van Duijneveldt, F. B.; van Duijneveldt-van de Rijdt, J. G. C. M.; van Lenthe, J. H. *Chem. Rev.* **1994**, *94*, 1873.
- (75) Gross, K. C. *Int. J. Quantum Chem.* **2001**, *85*, 569.
- (76) Pino, V.; Conde, F.; Ayala, J.; González, V.; Afonso, A. *Chromatographia* **2006**, *63*, 167.